Integrated Guidance and Feedback Control of Underactuated Robotics System in SE(3)

Sasi Prabhakaran Viswanathan, Amit K. Sanyal & Ehsan Samiei

Journal of Intelligent & Robotic Systems
with a special section on Unmanned Systems

ISSN 0921-0296
Volume 89
Combined 1-2

J Intell Robot Syst (2018) 89:251-263
DOI 10.1007/s10846-017-0547-0

J Intell Robot Syst (2018) 89:251–263
DOI 10.1007/s10846-017-0547-0

Integrated Guidance and Feedback Control of Underactuated Robotics System in SE(3)

Sasi Prabhakaran Viswanathan ·
Amit K. Sanyal · Ehsan Samiei

Received: 14 June 2016 / Accepted: 23 March 2017 / Published online: 7 April 2017

Abstract An integrated guidance and feedback control scheme for steering an underactuated vehicle through desired waypoints in three-dimensional space, is developed here. The underactuated vehicle is modeled as a rigid body with four control inputs. These control inputs actuate the three degrees of freedom of rotational motion and one degree of freedom of translational motion in a vehicle body-fixed coordinate frame. This actuation model is appropriate for a wide range of underactuated vehicles including spacecraft with internal attitude actuators, vertical take-off and landing (VTOL) aircraft, fixed-wing multirotor unmanned aerial vehicles (UAVs), maneuverable robotic vehicles, etc. The guidance problem is developed on the special Euclidean group of rigid body motions, SE(3), in the framework ofgeometric mechanics, which represents the vehicle dynamics globally on this configuration manifold. The integrated guidance and control algorithm selects the desired trajectory for the translational motion that passes through the given waypoints, and the desired trajectory for the attitude based on the desired thrust direction to achieve the translational motion trajectory. A feedback control law is then obtained to steer the underactuated vehicle towards the desired trajectories in translation and rotation. This integrated guidance and control scheme takes into account known bounds on control inputs and generates a trajectory that is continuous and at least twice differentiable, which can be implemented with continuous and bounded control inputs. The integrated guidance and feedback control scheme is applied to an underactuated quadcopter UAV to autonomously generate a trajectory through a series of given waypoints in SE(3) and track the desired trajectory in finite time. The overall stability analysis of the feedback system is addressed. Discrete time models for the dynamics and control schemes of the UAV are obtained in the form of Lie group variational integrators using the discrete Lagrange-d'Alembert principle. Almost global asymptotic stability of the feedback system over its state space is shown analytically and verified through numerical simulations.

S. P. Viswanathan
Akrobotix LLC, Syracuse, NY 13202, USA
e-mail: sasi@akrobotix.com

A. K. Sanyal (✉)
Faculty of Mechanical and Aerospace Engineering
at Syracuse University, Syracuse, NY 13244, USA
e-mail: aksanyal@syr.edu

E. Samiei
New Mexico State University, Las Cruces, NM, USA
e-mail: eh.samiei@gmail.com

Keywords Guidance · Navigation · Control · Underactuated system · Autonomous system · Finite time stability

1 Introduction

Autonomous operations of unmanned vehicles is considered an important topic of current research interest for several applications where remote human piloting is not feasible or convenient. Increased autonomy is useful in diverse applications like security, agriculture and aquaculture, inspection of civilian infrastructure, space and underwater exploration, wildlife tracking and conservation, package delivery and remote sensing. A critical aspect of reliable operations of unmanned vehicles is that of nonlinearly stable autonomous guidance and control with a large domain of attraction for robustness to external disturbances. This is particularly true for beyond visual-line-of-sight (BVLOS) operations that require safety and reliability in the presence of disturbances like wind. Absence of nonlinear stability in such a situation may lead to failure and crash of the vehicle, as shown in this video compilation. This paper investigates the problem of steering an underactuated vehicle that has four independent control inputs for the six degrees of freedom of translational and rotational motion in three dimensional Euclidean space. The control inputs actuate the three degrees of rotational motion and one degree of translational motion in a vehicle body-fixed coordinate frame. This actuation model covers a wide range of unmanned vehicles like fixed-wing and quadcopter unmanned aerial vehicles (UAVs), and spacecraft. An integrated guidance and feedback tracking control scheme is then obtained from a few given waypoints that are prescribed in terms of their position vectors. Prior related research on this topic includes [1, 2, 8, 9, 12, 14, 16, 17, 19, 23].

In addition to the necessity of a nonlinearly stable feedback control scheme with a large domain of attraction, the translational dynamics and attitude dynamics of the underactuated unmanned vehicle with the actuation described here, are coupled. As the control force vector is in a body-fixed direction, the body's rotational (attitude) dynamics needs to be controlled simultaneously with its translational dynamics. This motivates the approach used to design an integrated trajectory generation and feedback control system in this paper. The vehicle's pose (position and orientation) are represented globally and its dynamics analyzed in the framework of geometric mechanics [4, 7]. The configuration space is the Lie group SE(3) [13, 21, 22], which is the set of positions and orientations of the vehicle moving in three-dimensional Euclidean space. The integrated scheme given here uses a trajectory generation method that is similar to that of [14], in addition to an attitude control law that is almost globally finite-time stable (AGFTS) and a position tracking control law that is globally asymptotically stable. The AGFTS attitude tracking control law, in turn, is based on a recent approach to finite-time attitude stabilization on TSO(3) given in [5]. Because this control law uses the global and unique representation of rigid body attitude provided by rotation matrices, it is not ambiguous, unlike the quaternion representation, and it is free from kinematic singularities. The control laws assume that feedback from onboard sensors fixed to the vehicle, e.g., inertial and vision sensors, are available. Therefore, these control laws can be implemented with onboard sensors and state estimation schemes that can estimate the pose and body velocities from such sensor measurements [6, 10, 15, 20, 26]. In particular, the integrated guidance and control scheme given here can be used in conjunction with pose estimation schemes like [10, 11, 15] to provide autonomous navigation and control capability in GPS-denied environments.

This paper is organized as follows. Section 2 outlines the problem of generating a trajectory through given waypoints and provides the kinematics and dynamics model of the vehicle for arbitrary maneuvers. Section 3 details the trajectory generation and position feedback tracking control approaches for controlling the translational motion. The finite-time stable attitude tracking control law is provided in Section 4, along with the proof of stability of the overall feedback control system. Numerical simulation results based on a Lie group variational integration scheme to discretize the feedback dynamics, are provided in Section 6. A summary of results obtained in this paper and related research directions to be pursued in the near future are provided in Section 7.

2 Guidance Scheme

2.1 Coordinate Frame Definition

The configuration of an unmanned vehicle modeled as a rigid body is given by its position and orientation, which are together referred to as its pose. To define the pose of the vehicle, we fix a coordinate frame $\mathcal{B}$ to its body and another coordinate frame $\mathcal{I}$ that is fixed in space and takes the role of an inertial coordinate frame. Let $b \in \mathbb{R}^3$ denote the position vector of the origin of frame $\mathcal{B}$ with respect to frame $\mathcal{I}$ represented in frame $\mathcal{I}$. Let $R \in \mathrm{SO}(3)$ denote the orientation, defined as the rotation matrix from frame $\mathcal{B}$ to frame $\mathcal{I}$. The pose of the vehicle can be represented in matrix form as follows:

$$g = \begin{bmatrix} R & b \\ 0 & 1 \end{bmatrix} \in \mathrm{SE}(3), \tag{1}$$

where SE(3) is the six-dimensional Lie group of rigid body motions (translational and rotational) that is obtained as the semi-direct product of $\mathbb{R}^3$ with SO(3) [25].

2.2 Trajectory Generation for Unmanned Vehicle

The trajectory generation problem consists of creating an appropriately smooth trajectory through a given finite set of desired waypoints which the underactuated vehicle's trajectory is required to pass through. These waypoints are given in the inertial frame $\mathcal{I}$ as follows:

$$\begin{aligned} &b_{d_1}, b_{d_2}, \ldots, b_{d_n} \in \mathbb{R}^3, \ \text{ with } b_{d_i} = b_d(t_i) \in \mathbb{R}^3 \\ &\text{and } t_1 < t_2 < \ldots < t_n. \end{aligned} \tag{2}$$

Here $b_d(t)$ gives the desired position trajectory on $\mathbb{R}^3$ parameterized by time. A time trajectory for the position that is continuous and twice differentiable (i.e., $b_d(t) = \mathrm{C}^2(\mathbb{R}^3)$) could be generated, for example, using interpolating functions between the waypoints, e.g., [14, 17]. A time trajectory for the position can also be generated using standard linear quadratic control schemes, and we are currently exploring this approach to generate smooth trajectories between waypoints. Once the desired position trajectory over time has been generated based on the given waypoints, one needs to generate a desired attitude trajectory such that the position trajectory is achieved. The procedure by which this is done utilizes the known actuation and the dynamics model, and is detailed in the following section.

Let $g_d(t) \in \mathrm{SE}(3)$ be the desired pose (position, b_d and attitude, R_d) generated by the guidance scheme. Then the desired velocities (translational, ν_d and rotational, Ω_d) are given by $\xi_d(t)$ that satisfies the kinematics

$$\dot{g}_d(t) = g_d(t)\xi_d(t)^\vee, \quad \text{where } g_d(t) = \begin{bmatrix} R_d & b_d \\ 0 & 1 \end{bmatrix}, \tag{3}$$

$$\xi_d = \begin{bmatrix} \Omega_d \\ \nu_d \end{bmatrix} \in \mathbb{R}^6 \text{ and } \xi_d^\vee = \begin{bmatrix} \Omega_d^\times & \nu_d \\ 0 & 0 \end{bmatrix} \in \mathfrak{se} \subset \mathbb{R}^{4\times 4}.$$

Here $(\cdot)^\vee = \left\{ \begin{bmatrix} \Omega^\times & \nu \\ 0 & 0 \end{bmatrix} \in \mathfrak{se}(3) \mid \Omega, \nu \in \mathbb{R}^3 \right\}$, is a vector space isomorphism from $\mathbb{R}^6$ to the associated Lie algebra of SE(3), $\mathfrak{se}(3)$ and $(\cdot)^\times : \mathbb{R}^3 \to \mathfrak{so}(3) \subset \mathbb{R}^{3\times 3}$ is the skew-symmetric cross-product operator that gives the vector space isomorphism between $\mathbb{R}^3$ and $\mathfrak{so}(3)$:

$$x^\times = \begin{bmatrix} x_1 \\ x_2 \\ x_3 \end{bmatrix}^\times = \begin{bmatrix} 0 & -x_3 & x_2 \\ x_3 & 0 & -x_1 \\ -x_2 & x_1 & 0 \end{bmatrix}. \tag{4}$$

In addition to the desired waypoints, the vehicle has to satisfy its known dynamics. Consider the "nominal" model of the dynamics for the underactuated vehicle as given by

$$\mathbb{I}\dot{\xi} = \mathrm{ad}_\xi^* \mathbb{I}\xi + \varphi(g, \xi) + Bu, \ u \in \mathcal{C} \subset \mathbb{R}^4, \ B \in \mathbb{R}^{6\times 4}, \tag{5}$$

where $\mathbb{I}$ denotes the mass (m) and inertia (J) properties of the vehicle given as

$$\mathbb{I} = \begin{bmatrix} J & 0 \\ 0 & mI_3 \end{bmatrix} \in \mathbb{R}^{6\times 6} \tag{6}$$

and I_3 is the 3×3 identity matrix.

The vector of known (modeled) moments and forces is denoted $\varphi(g, \xi) \in \mathbb{R}^6$; usually this is obtained from a known model. Note that the vehicle has four inputs for the six degrees of freedom of translational and rotational motion, as given by the control influence matrix B, which can be expressed in block matrix form as follows:

$$B = \begin{bmatrix} I_4 \\ 0_{2\times 4} \end{bmatrix},$$

where I_4 is the 4×4 identity matrix. The adjoint operator on $\mathfrak{se}(3)$ and the co-adjoint operator (ad^*_ξ) are defined in matrix form [25] as

$$\mathrm{ad}_\xi = \begin{bmatrix} -\Omega^\times & 0 \\ -\nu^\times & -\Omega^\times \end{bmatrix} \text{and } \mathrm{ad}^*_\xi = (\mathrm{ad}_\xi)^{\mathrm{T}}, \tag{7}$$

where $\Omega, \nu \in \mathbb{R}^3$ denote the rotational and translational velocities of the underactuated vehicle, respectively, in frame $\mathcal{B}$. The vector of control inputs $u \in \mathcal{C} \subset \mathbb{R}^4$ has to be in the set of admissible controls $\mathcal{C}$ and directly actuates the three degrees of rotational motion and one degree of translational motion. This actuation model is applicable to aerial, space and underwater vehicles and it is known that a rigid body is controllable with such actuation [8, 12].

3 Feedback Guidance and Tracking on TSE(3)

The desired trajectory is generated in SE(3) and the tracking errors are expressed with respect to inertial and body fixed frames as follows,

$\tilde{b} := b - b_d$	Position tracking error in inertial frame
$x := R_d^{\mathrm{T}}\tilde{b}$	Position tracking error in body fixed frame
$\tilde{v} := v - v_d = \dot{\tilde{b}}$	Velocity tracking error in inertial frame
$Q := R_d^{\mathrm{T}} R$	Attitude tracking error
$\omega := \Omega - Q^{\mathrm{T}}\Omega_d$	Angular velocity tracking error

3.1 Tracking errors expressed in body frame

Tracking errors on TSE(3) are defined as follows (as in [22]):

$$g = \begin{bmatrix} R & b \\ 0 & 1 \end{bmatrix}, g_d = \begin{bmatrix} R_d & b_d \\ 0 & 1 \end{bmatrix}. \tag{8}$$

Tracking error on SE(3):

$$h = g_d^{-1} g = \begin{bmatrix} Q & x \\ 0 & 1 \end{bmatrix}, \tag{9}$$

where $Q = R_d^{\mathrm{T}} R$ and $x = R_d^{\mathrm{T}}(b - b_d) = R_d^{\mathrm{T}}\tilde{b}$. Therefore, the kinematics for the pose tracking error is:

$$\dot{h} = h\xi^\vee, \tag{10}$$

where

$$\xi^\vee = \begin{bmatrix} \omega^\times & \upsilon \\ 0 & 0 \end{bmatrix}, \tag{11}$$

and $\omega = \Omega - Q^{\mathrm{T}}\Omega_d$, $\upsilon = \nu - Q^{\mathrm{T}}(\nu_d + \Omega_d^\times x)$. The dynamics for the tracking errors in velocities is:

$$\begin{aligned} m\dot{\upsilon} = & -fe_3 + m\{\omega^\times Q^{\mathrm{T}}\nu_d - Q^{\mathrm{T}}(\dot{\nu}_d + \dot{\Omega}_d^\times x \\ & +\Omega_d^\times Q\upsilon))\} + m(\upsilon + Q^{\mathrm{T}}\nu_d)^\times(\omega + Q^{\mathrm{T}}\Omega_d) \\ & +mgQ^{\mathrm{T}}R_d^{\mathrm{T}}e_3, \end{aligned} \tag{12}$$

$$\begin{aligned} J\dot{\omega} = & \tau + J(\omega^\times Q^{\mathrm{T}}\Omega_d - Q^{\mathrm{T}}\dot{\Omega}_d) \\ & -(\omega + Q^{\mathrm{T}}\Omega_d)^\times J(\omega + Q^{\mathrm{T}}\Omega_d). \end{aligned} \tag{13}$$

3.2 Translational Motion Control in Inertial Frame

Because the desired position trajectory, $b_d(t)$, is generated in the inertial frame $\mathcal{I}$, it is convenient to express the position and translational velocity tracking error dynamics (12) in this frame. As the translational dynamics is expressed in the inertial frame, the rotational dynamics is decoupled from the translational dynamics such that the translation control force is obtained in the inertial frame followed by the appropriate attitude control in body-fixed frame to track the desired trajectory, b_d. Note that $v = R\nu$ and $Q^{\mathrm{T}}\nu_d = RR_d\nu_d = R^{\mathrm{T}}v_d$, where $v_d = R_d\nu_d = \dot{b}_d$. Define $\tilde{b} := b - b_d$ and $\tilde{v} := v - v_d = \dot{\tilde{b}}$. Therefore, in inertial frame $\mathcal{I}$, the position and translational velocity tracking error dynamics are:

$$\dot{\tilde{b}} = \tilde{v} = v - v_d, \quad m\dot{\tilde{v}} = mge_3 - fr_3 + m\dot{v}_d, \tag{14}$$

where $r_3 = Re_3$ is the third column vector of the rotation matrix R from frame $\mathcal{B}$ to frame $\mathcal{I}$, which represents the true attitude of the body. Here, $e_1 = [1\ 0\ 0]^{\mathrm{T}}$, $e_2 = [0\ 1\ 0]^{\mathrm{T}}$ and $e_3 = [0\ 0\ 1]^{\mathrm{T}}$ are the standard basis vectors (as column vectors) of $\mathbb{R}^3$. Note that $fr_3 = \bar{\varphi}_c$ can be considered as the control force vector acting on the body, expressed in inertial frame. The magnitude of this vector is one of the control inputs f, which is designed as a feedback control law. The direction of this vector $r_3 = Re_3$ is designed as part of the desired trajectory for the attitude in SO(3), with the other two column vectors of the rotation matrix R obtained from the generated trajectory for r_3. This feedback guidance plus trajectory tracking control is detailed in the following development.

Consider the following Lyapunov function for the desired translational motion:

$$V_{tr}(\tilde{b}, \tilde{v}) = \frac{1}{2}m\tilde{v}^{\mathrm{T}}\tilde{v} + \frac{1}{2}\tilde{b}P\tilde{b}, \tag{15}$$

where $P \in \mathbb{R}^{3\times 3}$ is a positive definite control gain matrix. Therefore, along the translational error dynamics (14),

$$\begin{aligned}\dot{V}_{tr} &= m\tilde{v}^{\mathrm{T}}\dot{\tilde{v}} + \tilde{b}P\dot{\tilde{b}} = \tilde{v}^{\mathrm{T}}(m\dot{\tilde{v}} + P\tilde{b}) \\ &= \tilde{v}^{\mathrm{T}}(mge_3 - fr_3 - m\dot{v}_d + P\tilde{b}).\end{aligned} \tag{16}$$

It is desired that the control force vector satisfies

$$fr_3 = \bar{\varphi}_c = mge_3 + P\tilde{b} + L_v\tilde{v} - m\dot{v}_d, \tag{17}$$

where $L_v \in \mathbb{R}^{3\times 3}$ is another positive definite control gain matrix. Therefore, the control law for the magnitude of this force vector is:

$$f = e_3^{\mathrm{T}}R^{\mathrm{T}}\bar{\varphi}_c = e_3^{\mathrm{T}}R^{\mathrm{T}}\big(mge_3 + P\tilde{b} + L_v(Rv - v_d) - m\dot{v}_d\big). \tag{18}$$

However, to achieve stable tracking of the desired translational motion, the attitude has to be controlled such that the direction of $Re_3 = r_3$ agrees with that specified by Eq. 17. This is done in the following subsection.

3.3 Generating Desired Attitude Trajectory

Given the desired control force vector in inertial frame as given by Eq. 17, one can generate a desired trajectory for the third column of R_d (the desired attitude) as follows:

$$r_{3d} = \frac{mge_3 + P\tilde{b} + L_v\tilde{v} - m\dot{v}_d}{\left\|mge_3 + P\tilde{b} + L_v\tilde{v} - m\dot{v}_d\right\|} = R_d e_3. \tag{19}$$

Select an appropriate $s_d(t) \in \mathcal{C}^2(\mathbb{R}^3)$ such that it is transverse to r_{3d}. Now compute

$$r_{2d} = \frac{r_{3d} \times s_d}{||r_{3d} \times s_d||} = R_d e_2,$$

$$\text{and } r_{1d} = r_{2d} \times r_{3d} = R_d e_1. \tag{20}$$

The desired attitude trajectory is then given by:

$$R_d = [r_{2d} \times r_{3d} r_{2d} r_{3d}] \in \mathrm{SO}(3). \tag{21}$$

Few methods to select $s_d(t)$ appropriately is described in the following results.

Proposition 1 *If s_d is selected as*

$$s_d = \mathbb{1} \times r_{3d} + \mu e_1, \ \text{ with } \mu > 3, \tag{22}$$

then s_d is always transverse and never parallel to r_{3d}.

Proof The condition on μ in Eq. 22 comes from the following observation:

$$\begin{aligned} r_{3d} \times s_d &= r_{3d} \times (\mathbb{1} \times r_{3d} + \mu e_1) \\ &= (r_{3d}^{\mathrm{T}} r_{3d})\mathbb{1} - (r_{3d}^{\mathrm{T}}\mathbb{1})r_{3d} + \mu r_{3d} \times e_1 \\ &= \mathbb{1} - (r_{3d}^{\mathrm{T}}\mathbb{1})r_{3d} + \mu r_{3d} \times e_1, \end{aligned} \tag{23}$$

because $r_{3d} \in \mathbb{S}^2$, i.e., it is a unit vector. Define $\rho(r_{3d}) = \mathbb{1} - (r_{3d}^{\mathrm{T}}\mathbb{1})r_{3d}$ so that

$$r_{3d} \times s_d = \rho(r_{3d}) + \mu r_{3d} \times e_1. \tag{24}$$

It can be verified that the components of the vector $\rho(r_{3d})$ are bounded in the closed interval $[-\frac{4}{3}, 0]$. Therefore, the first component of the vector $r_{3d} \times s_d$ is bounded in the closed interval $[\mu - \frac{4}{3}, \mu]$. If $\mu > 3$, then this component is always positive, and therefore $r_{3d} \times s_d \neq 0$. Therefore, the choice of s_d given in Eq. 22 ensures that it is always transverse to the generated r_{3d}. □

The following statement gives a simpler choice of s_d in $\mathbb{R}^3$ that is transverse to $r_{3d} \in \mathbb{R}^3$. It also gives a vector that is orthogonal to the given unit vector.

Proposition 2 *Let $r_{3d} = \begin{bmatrix} a_1 & a_2 & a_3 \end{bmatrix}^{\mathrm{T}} \in \mathbb{S}^2 \subset \mathbb{R}^3$ be a known unit vector as given in* Eq. 19. *The vector*

$$s_d = \begin{bmatrix} a_2 + a_3 \\ a_3 - a_1 \\ -a_1 - a_2 \end{bmatrix} \tag{25}$$

is orthogonal to r_{3d}.

Proof This is easily verified by the property of scalar product (orthogonal projection) as follows:

$$\begin{aligned} r_{3d}^{\mathrm{T}} s_d &= a_1(a_2 + a_3) + a_2(a_3 - a_1) + a_3(-a_1 - a_2) \\ &= a_1(a_2 + a_3 - a_2 - a_3) + a_2(a_3 - a_3) = 0. \end{aligned}$$

This shows that the vector s_d as defined by Eq. 25 is orthogonal to the given vector r_{3d}. □

As the next step, a control torque is selected such that $R \to R_d$ in finite time; this is done using an attitude tracking control scheme outlined in the next section.

4 Feedback Tracking Control Schemes

The finite-time attitude tracking control scheme given here is based on the recent work [5]. It is known that finite-time stability is more robust to external disturbances to the dynamics than asymptotic or exponential stability [3, 5]. Having a finite-time stable attitude control scheme also theoretically guarantees that the overall combined feedback attitude and position tracking control scheme is asymptotically stable, unlike the schemes presented in [14] which only guarantee convergence and not stability. This is because the desired thrust direction required for the position control is achieved in finite time, as shown in the second part of this section. The first part of this section details the attitude tracking control scheme and its stability properties, while the second part gives the stability result for the entire (translational and rotational) motion control scheme.

4.1 Finite-time Stable Attitude Tracking Control on TSO(3)

Here we provide a finite-time stable attitude control scheme that is continuous and can be implemented with actuators commonly used for unmanned vehicles like rotorcraft and fixed-wing UAVs. The following two lemmas are used to prove the main result.

Lemma 1 *Let a and b be non-negative real numbers and let $p \in (1, 2)$. Then*

$$a^{(1/p)} + b^{(1/p)} \geq (a + b)^{(1/p)}. \tag{26}$$

This inequality is strict if both a and b are non-zero.

This above inequality holds for all $p > 1$ as $f(x) = x^{(1/p)}$ is a concave function and therefore subadditive. For the finite-time attitude tracking scheme, only the case where $p \in (1, 2)$ is required.

Lemma 2 *Let $K = \mathrm{diag}(k_1, k_2, k_3)$, where $k_1 > k_2 > k_3 \geq 1$. Define*

$$s_K(Q) = \sum_{i=1}^{3} k_i (Q^{\mathrm{T}} e_i) \times e_i, \tag{27}$$

such that $\frac{\mathrm{d}}{\mathrm{d}t}\langle K, I - Q\rangle = \omega^{\mathrm{T}} s_K(Q)$. Here $\langle A, B\rangle = \mathrm{tr}(A^{\mathrm{T}} B)$, which makes $\langle K, I - Q\rangle$ a Morse function defined on $\mathrm{SO}(3)$. Let $\mathcal{S} \subset \mathrm{SO}(3)$ be a closed subset containing the identity in its interior, defined by

$$\begin{aligned} \mathcal{S} = \big\{ Q \in \mathrm{SO}(3) \ : \ Q_{ii} \geq 0 \text{ and } Q_{ij} Q_{ji} \leq 0 \\ \forall i, j \in \{1, 2, 3\}, \ i \neq j \big\}. \end{aligned} \tag{28}$$

Then for $Q \in \mathcal{S}$, we have

$$s_K(Q)^T s_K(Q) \geq \mathrm{tr}(K - KQ). \tag{29}$$

The proof of this result is given in [5], and is omitted here for brevity. The finite-time attitude tracking control scheme and its proof of stability are given as follows. Note that this control scheme is continuous (indeed smooth) in time. This is unlike sliding mode control schemes that cannot be implemented with actuators (like rotors) that can only provide continuous control inputs.

Theorem 1 *Consider the attitude dynamics of* Eq. 13 *with $s_K(Q)$ as defined in* Eq. 27. *Define*

$$z_K(Q) = \frac{s_K(Q)}{\left(s_K^{\mathrm{T}}(Q) s_K(Q)\right)^{1-1/p}}, \text{ and} \tag{30}$$

$$w(Q, \omega) = \frac{\mathrm{d}}{\mathrm{d}t} s_K(Q) = \sum_{i=1}^{3} k_i e_i \times (\omega \times Q^{\mathrm{T}} e_i), \tag{31}$$

where p is as defined in Lemma 1. Further, let L_Ω be a positive definite control gain matrix such that $L_\Omega - J$

is positive semidefinite, let $k_p > 1$ and define κ such that

$$\kappa^p = \frac{\sigma_{L,\min}}{\sigma_{J,\max}} > 0.$$

Consider the feedback control law for τ given by

$$\tau = J\left(Q^{\mathrm{T}}\dot{\Omega}_d - \frac{\kappa H(s_K(Q))}{\left(s_K^{\mathrm{T}}(Q)s_K(Q)\right)^{1-1/p}} w(Q,\omega)\right) +(Q^{\mathrm{T}}\Omega_d)^{\times} J\left(Q^{\mathrm{T}}\Omega_d - \kappa z_K(Q)\right) + \kappa J\left(z_K(Q) \times Q^{\mathrm{T}}\Omega_d\right) + \kappa J(\omega + Q^{\mathrm{T}}\Omega_d)\times z_K(Q) - k_p s_K(Q) - \frac{L_\Omega \Psi(Q,\omega)}{\left(\psi(Q,\omega)^{\mathrm{T}} L_\Omega \Psi(Q,\omega)\right)^{1-1/p}}, \tag{32}$$

where

$$\psi(Q,\omega) = \omega + \kappa z_K(Q), \tag{33}$$

$$\text{and } H(x) = I - \frac{2(1-1/p)}{x^{\mathrm{T}}x} x x^{\mathrm{T}}. \tag{34}$$

Then the feedback attitude tracking error dynamics given by Eq. 13 *is stabilized to $(Q,\omega) = (I,0)$ in finite time.*

Proof Consider $\omega = -\kappa z_K(Q)$ and define the Morse-Lyapunov function $\langle K, I-Q\rangle$ on SO(3). Then the time derivative of this Morse-Lyapunov function along the attitude kinematics is given by

$$\begin{aligned}\frac{\mathrm{d}}{\mathrm{d}t}\langle K, I-Q\rangle &= \omega^{\mathrm{T}} s_K(Q) = -\kappa s_K^{\mathrm{T}}(Q) z_K(Q) \\ &= -\kappa \frac{s_K^{\mathrm{T}}(Q)s_K(Q)}{\left(s_K^{\mathrm{T}}(Q)s_K(Q)\right)^{1-1/p}} \\ &= -\kappa\left(s_K^{\mathrm{T}}(Q)s_K(Q)\right)^{1/p} \\ &\le -\kappa\left(\langle K, I-Q\rangle\right)^{1/p},\end{aligned} \tag{35}$$

where we employed inequality (26) in Lemma 1. Therefore, when $\Psi(Q,\omega)=0$, one can conclude that $\langle K, I-Q\rangle \to 0$ in finite time for all initial Q in the subset $\mathcal{S} \subset$ SO(3) defined in Lemma 2, which yields $Q \to I$ in finite time once $Q \in \mathcal{S}$.

The control law is then designed to ensure that $\Psi(Q,\omega) \to 0$ in finite time. Consider the Lyapunov function

$$V_{rot}(Q,\omega) = k_p\langle K, I-Q\rangle + \Psi(Q,\omega)^{\mathrm{T}} J \Psi(Q,\omega), \tag{36}$$

for the attitude dynamics of Eq. 13 with control law (32). The time derivative of this Lyapunov function along this feedback dynamics is given by

$$\begin{aligned}\dot{V}_{rot} &= k_p\omega^{\mathrm{T}} s_K(Q) + \psi(Q,\omega)^{\mathrm{T}} J\dot{\psi}(Q,\omega) \\ &= k_p\omega^{\mathrm{T}} s_K(Q) + \Psi^{\mathrm{T}}\Big[\tau_c + J\Omega \times \big(Q^{\mathrm{T}}\Omega_d \\ &\quad -\kappa z_K(Q)\big) + J\big(\omega^{\times} Q^{\mathrm{T}}\Omega_d - Q^{\mathrm{T}}\dot{\Omega}_d\big) \\ &\quad + \frac{\kappa J H(s_K(Q))}{\left(s_K^{\mathrm{T}}(Q)s_K(Q)\right)^{1-1/p}} w(Q,\omega)\Big]\end{aligned} \tag{37}$$

After substituting the control law (32) into the expression (37) and carrying out several algebraic simplifications, one obtains

$$\begin{aligned}\dot{V}_{rot} &= -k_p\kappa\left(s_K(Q)^{\mathrm{T}} s_K(Q)\right)^{1/p} \\ &\quad -\left(\Psi(Q,\omega)^{\mathrm{T}} L_\Omega \Psi(Q,\omega)\right)^{1/p} \\ &\le -\kappa\left(k_p\langle K, I-Q\rangle\right)^{1/p} \\ &\quad -\kappa\left(\Psi(Q,\omega)^{\mathrm{T}} J \Psi(Q,\omega)\right)^{1/p},\end{aligned}$$

for $(Q,\omega) \in \mathcal{S} \times \mathbb{R}^3$, where $\mathcal{S} \subset$ SO(3) is as defined in (28). After substituting inequality (26) into the above expression, one obtains

$$\begin{aligned}\dot{V}_{rot} &\le -\kappa\left(k_p\langle K, I-Q\rangle + \Psi(Q,\omega)^{\mathrm{T}} J \Psi(Q,\omega)\right)^{1/p} \\ &= -\kappa V_{rot}^{1/p},\end{aligned} \tag{38}$$

which implies that the feedback attitude tracking control system is (locally) finite-time stable at $(Q,\omega) = (I,0)$ [3].

Note that the domain of attraction shown in the above analysis is $(Q,\omega) \in \mathcal{S} \times \mathbb{R}^3$. The rest of the proof to show almost global finite-time stability of the attitude feedback control is identical to the proof of the similar result given in [5], and is omitted here for the sake of brevity. □

4.2 Stability of the Overall Feedback System on TSE(3)

The following statement outlines the stability of the overall feedback system with the control laws (32) and (18).

Theorem 2 *The overall feedback control system given by the tracking error kinematics* (10) *and dynamics* (13)–(14) *is asymptotically stable for the generated state trajectory $\big(b_d(t), R_d(t), v_d(t), \Omega_d(t)\big) \subset$ TSE(3). Moreover, the domain of convergence is almost global over the state space.*

Proof This attitude tracking control scheme given by Theorem 1 ensures that $R(t) = R_d(t)$ for time $t \geq T$ where $T > 0$ is finite. Therefore, one obtains $r_3 = Re_3 = r_{3d}$ for $t \geq T$, and from Eqs. 18 and 19,

$$f = \left\| mge_3 + P\tilde{b} + L_v\tilde{v} - m\dot{v}_d \right\|, \text{ and}$$

$$fr_3 = fr_{3d} = mge_3 + P\tilde{b} + L_v\tilde{v} - m\dot{v}_d \text{ for } t \geq T. \tag{39}$$

Substituting Eqs. 39 in 16 gives:

$$\begin{aligned}\dot{V}_{tr} &= \tilde{v}^{\mathrm{T}}(mge_3 - fr_{3d} - m\dot{v}_d + P\tilde{b}) \\ &= -\tilde{v}^{\mathrm{T}} L_v \tilde{v} \leq 0. \end{aligned} \tag{40}$$

Since L_v is positive definite, $\dot{V}_{tr} = 0$ if and only if $\tilde{v} = 0$. Applying LaSalle's invariance principle, one can show that when $\tilde{v} = 0$, $m\dot{\tilde{v}} = mge_3 - fr_{3d} + m\dot{v}_d = 0$, and therefore $P\tilde{b} = 0$, and thus $\tilde{b} = 0$. Therefore, the tracking errors for the translational motion converge to $(\tilde{b}, \tilde{v}) = (0, 0)$. □

Note that the finite-time stability of the attitude control scheme guarantees that the desired thrust direction, r_{3d}, is achieved in finite time. This in turn ensures that the desired position trajectory is asymptotically tracked and the overall attitude and position tracking control system is asymptotically stable. The almost global domain of convergence also provides robustness to disturbances, as shown in [5]. Moreover, the continuous control schemes give here can be implemented with rotorcraft UAV that have actuators that can only provide continuous control forces and torques.

5 Application to Autonomous UAV Navigation

5.1 Actuation Model

A vertical take-off and landing (VTOL) quadrotor/quadcopter UAV model with four identical actuators (propellers), each separated by a scalar distance D from the axis of rotation of the actuators to the center of the UAV, is considered here. A conceptual diagram of guidance on SE(3) through a set of waypoints is given in Fig. 1.

The continuous equations of motion of the quadcopter UAV is written as,

$$\dot{R} = R\,\Omega^{\times}, \tag{41}$$

$$m\,\dot{v} = m\,g\,R^{\mathrm{T}} e_3 - f\,e_3, \tag{42}$$

$$J\dot{\Omega} = J\Omega \times \Omega + \tau \tag{43}$$

Each propeller can generate a thrust f_i proportional to the square of the corresponding motor speed i.e., $f_i = k_f \bar{\omega}_i^2$, and the torque generated by each actuator is directly proportional to its thrust i.e., $\tau_i = k_\tau \bar{\omega}_i^2$. The first and second axes (a_1 and a_2) of the body-fixed frame $\mathcal{B}$ lie in the plane normal to the axes of the propellers. The total thrust, $f = \sum_{i=1}^{4} f_i$ acts along the third axis $-a_3$ of the body-fixed frame $\mathcal{B}$. For such an UAV as shown in Fig. 1, the control input vector $u = \begin{bmatrix} f & \tau \end{bmatrix}^{\mathrm{T}}$ can be expressed in terms of the actuator speeds $\bar{\omega}_i$ according to

$$u = \mathcal{K} \begin{bmatrix} \bar{\omega}_1^2 & \bar{\omega}_2^2 & \bar{\omega}_3^2 & \bar{\omega}_4^2 \end{bmatrix}^{\mathrm{T}},$$

where

$$\mathcal{K} = \begin{bmatrix} -k_f & -k_f & -k_f & -k_f \\ 0 & -k_f D & 0 & k_f D \\ k_f D & 0 & -k_f D & 0 \\ -k_\tau & k_\tau & -k_\tau & k_\tau \end{bmatrix} \in \mathbb{R}^{4\times 4}$$

is a constant invertible matrix for $k_f \neq 0$ and $k_\tau \neq 0$ [24]. Then,

$$\begin{bmatrix} \bar{\omega}_1^2 \\ \bar{\omega}_2^2 \\ \bar{\omega}_3^2 \\ \bar{\omega}_4^2 \end{bmatrix} = \mathcal{K}^{-1} \begin{bmatrix} f \\ \tau \end{bmatrix} \tag{44}$$

5.2 Guidance Algorithm

The objective of the integrated trajectory generation and control is to navigate the UAV from an initial pose to a final desired pose in SE(3), through a finite set of desired waypoints. Pseudocode of the integrated guidance and feedback control algorithm that generates a trajectory that passes through the waypoints (2) and satisfies the kinematics and dynamics (3)–(5) is given below:

Algorithm 1 Integrated Guidance and Feedback Control

---

procedure IGFC(b_d, f, R_d, τ) $\triangleright$ b_d and f are in $\mathcal{I}$
  set $\mathcal{I}$ $\triangleright$ Fix the inertial frame
  $b = \begin{bmatrix} b_x & b_y & b_z \end{bmatrix}^{\mathrm{T}}$ $\triangleright$ Initialize the UAV with respect to an inertial frame $\mathcal{I}$
  Select $b_{d_1}, b_{d_2}, \ldots, b_{d_n}$ $\triangleright$ select desired waypoints in $\mathbb{R}^3$
  Generate $b_d(t) = \mathrm{C}^2(\mathbb{R}^3)$ $\triangleright$ Generate a smooth trajectory as a function of time in $\mathcal{I}$
  while $t > t_0$ **do**
    $f \leftarrow (18)$ $\triangleright$ Compute the UAV control thrust in $\mathcal{I}$
    $r_3d \leftarrow (19)$ $\triangleright$ desired thrust vector direction in the inertial frame
    for $s_d(t) \in \mathcal{C}^2(\mathbb{R}^3)$ **do** $s_d \pitchfork r_{3d}$
      $r_{2d} \leftarrow (20)$
    end for
    $R_d \leftarrow \begin{bmatrix} r_{2d} \times r_{3d} r_{2d} r_{3d} \end{bmatrix}$ $\triangleright$ Generate the desired attitude trajectory
    $\tau \leftarrow (32)$ $\triangleright$ Compute attitude control torque such that $R(t) \to R_d(t)$ in finite time
  end while
  return (b, R, ν) $\triangleright$ Implement the integrated guidance and feedback control on TSE(3) with feedback of (b, R, ν) and knowledge of $(b_d, v_d, \dot{v}_d, R_d, \Omega_d, \dot{\Omega}_d)$
end procedure

---

6 Numerical Validation

6.1 Discretization of the UAV Dynamics

The continuous equations of motion are discretized in the form of Lie Group Variational Integrator (LGVI) for digital implementation by applying the discrete Lagrange-d'Alembert principle. The LGVI preserves the structure of the configuration space, which in this case is the Lie group SE(3), without any reprojection or parametrization. The LGVI schemes also have good energy-momentum properties when the dynamical model is that of a conservative or nearly conservative system. The discrete model we obtain is a Lie group variational integrator similar to the ones obtained in [18].

Let $h \neq 0$ denote the fixed time step size, such that $h = t_{k+1} - t_k$. Then the discretized equations of motion obtained in the form of LGVI as,

$$
\begin{aligned}
R_{k+1} &= R_k F_k, \\
b_{k+1} &= h\, R_k \nu_k + b_k, \\
m\nu_{k+1} &= m\, F_k^{\mathrm{T}} \nu_k + h\, m\, g\, R_{k+1}^{\mathrm{T}} e_3 - h\, f_k\, e_3, \\
\Omega_{d_{k+1}}^{\times} &= \frac{1}{h} \log(R_{d_k}^{\mathrm{T}} R_{d_{k+1}}), \\
J\,\Omega_{k+1} &= F_k^{\mathrm{T}}\, J \Omega_k + h \tau_k,
\end{aligned} \tag{45}
$$

where $F_k \approx \exp(h\, \Omega_k^{\times}) \in \mathrm{SO}(3)$ guarantees that R_k evolves on SO(3).

6.2 Simulation Results

The integrated guidance and feedback control scheme is numerical simulated for an UAV quadcopter of mass, $m = 4.34$ kg; $J = \mathrm{diag}[0.820\ 0.0845\ 0.1377]\mathrm{kgm}^2$. The helical desired trajectory and the initial conditions are given as follows

$$
\begin{aligned}
b_d(t) &= \begin{bmatrix} 0.4\sin(\pi t) & 0.6\cos(\pi t) & 0.4\,t \end{bmatrix}^{\mathrm{T}}, \\
b(0) &= \begin{bmatrix} 1 & 0 & 0 \end{bmatrix}^{\mathrm{T}}, \\
R(0) &= I, \\
v(0) &= \begin{bmatrix} 0 & 0 & 0 \end{bmatrix}^{\mathrm{T}};\ \dot{v}(0) = \begin{bmatrix} 0 & 0 & 0 \end{bmatrix}^{\mathrm{T}} \text{ and} \\
\Omega(0) &= \begin{bmatrix} 0 & 0 & 0 \end{bmatrix}^{\mathrm{T}}.
\end{aligned}
$$

The numerical simulation is performed for five seconds, $t = 5$ with a time step size of $h = 0.01$, using the LGVI routine given in Eq. 45 for the choice of s_d as given in Proposition 1. The results of the numerical simulation are summarized in Fig. 4. The attitude error function Φ is parametrized as principle rotation angle, in terms of Q as given by,

$$
\Phi = \cos^{-1}\left(\frac{1}{2}(\mathrm{tr}(Q) - 1)\right).
$$

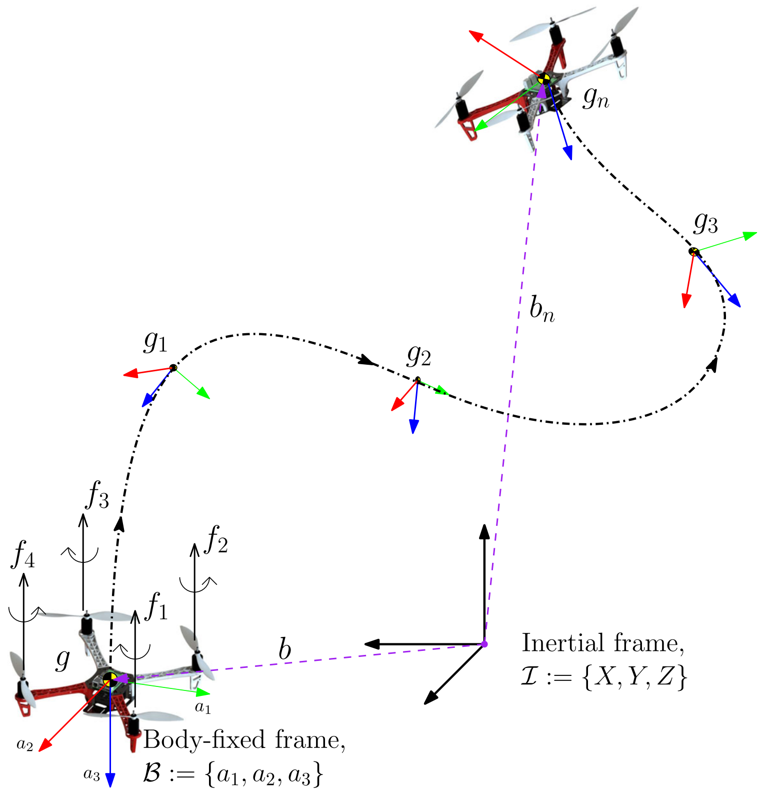

Fig. 1 Guidance through a set of finite waypoints between initial and final configurations on SE(3)

The numerical results are obtained after selecting the following gain values:

$$P = 38 \times I^{3\times3}; L_v = 25 \times I^{3\times3}$$

$$L_\Omega = 3.5 \times I^{3\times3}; p = 0.75; \kappa = 0.04 \text{ and } k_p = 4.5.$$

These gain values were selected after trial and error, and provide desirable transient response characteristics of the overall control scheme.

The time trajectory of the UAV tracking the desired trajectory is shown in Fig. 2 and it is inferred that the trajectory converges to the desired values in finite

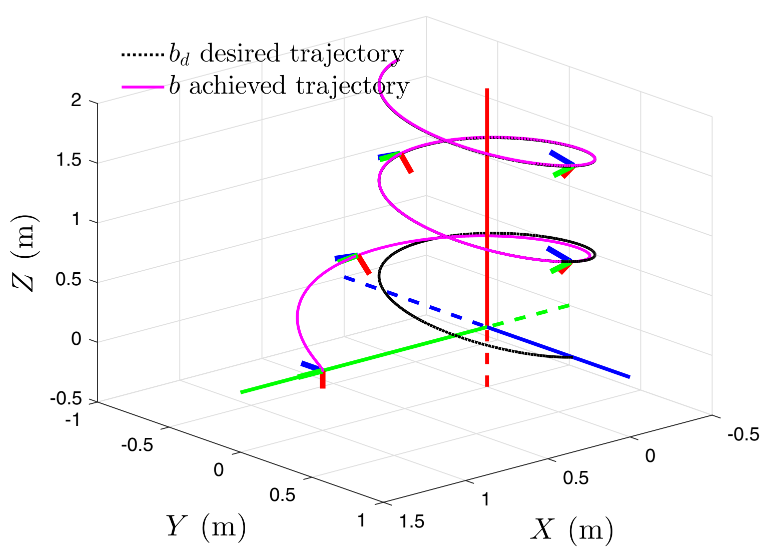

Fig. 2 Time trajectory of an UAV tracking the desired trajectory, b_d

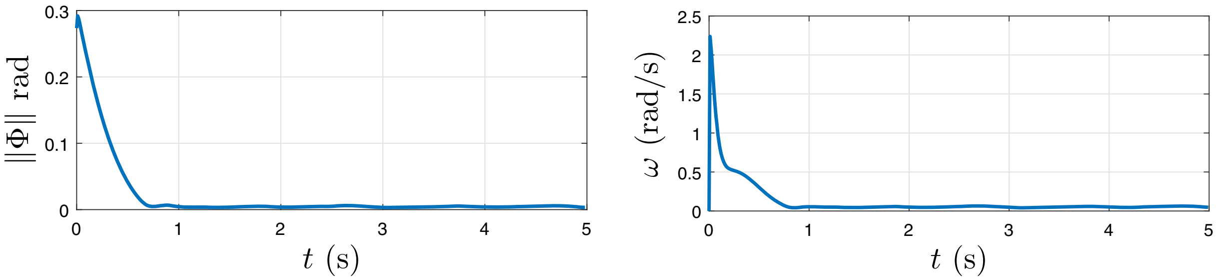

(a) Attitude tracking error function (b) Angular velocity error, ω

Fig. 3 Attitude and angular velocity error for the helical maneuver of an UAV

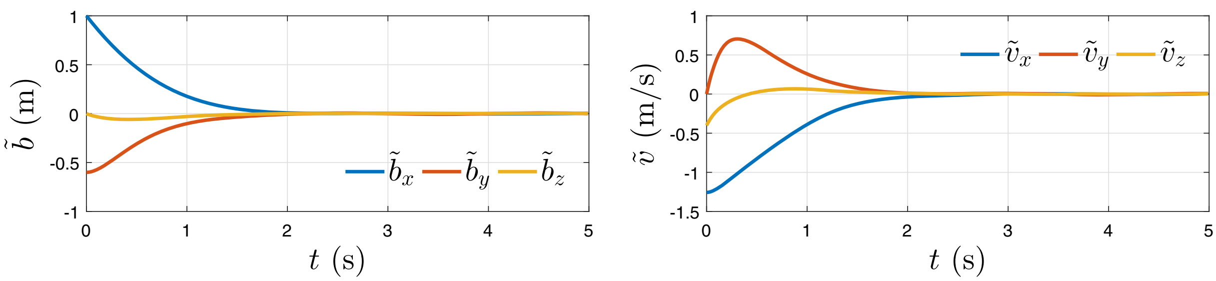

(a) Position tracking error (b) Velocity tracking error

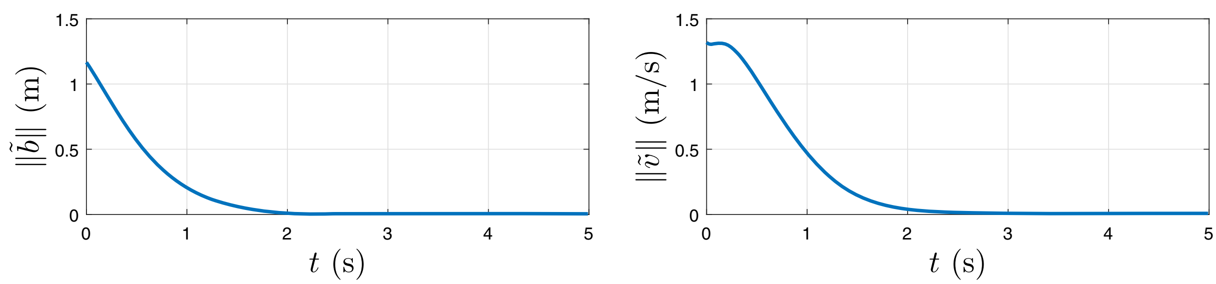

(c) Norm of position tracking error (d) Norm of velocity tracking error

Fig. 4 Position and velocity tracking response of the underactuated UAV

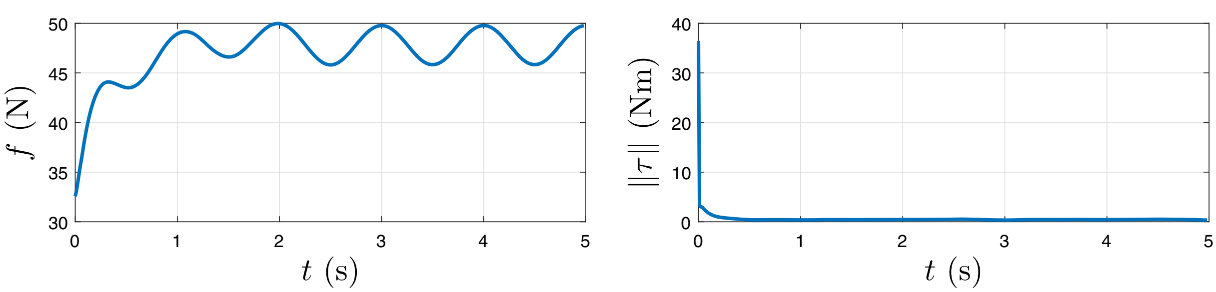

(a) Magnitude of total thrust (b) Control Torque

Fig. 5 Control effort

time and remains stable for all time, $t > 0$. The attitude tracking error given by the principal angle, Φ converges in finite time which indicates that R tracks R_d as shown in Fig. 3a. The angular velocity error is plotted in Fig. 3b, and it is shown to converge to a small bounded neighborhood of the origin. The position and velocity tracking response of the control law given by Eq. 18 is shown in Fig. 4. The stable position tracking performance is shown in Fig. 4a and b, which show the position tracking errors converging to zero and therefore the control scheme presented here tracks the position and remains stable even with the large initial position error. The control scheme also ensures the UAV tracks the translation velocity as shown in Fig. 4b and d. The control efforts are shown to be within reasonable bounds and practically achievable for multirotor UAVs. The total magnitude of the thrust force is less than 50 Newtons as shown in Fig. 5a and the corresponding control torque is shown in Fig. 5b; these control inputs are reasonable and within the capabilities of the four propellers of the UAV as given by Eq. 44. From the simulation results, it can be inferred that the integrated guidance and control scheme takes the UAV from an initial pose to a desired final pose in SE(3) and the overall feedback system is stable.

7 Conclusion

An integrated trajectory generation and feedback tracking control scheme for a rigid body with one actuated translational degree of freedom and all three rotational degrees of freedom actuated, is presented here. This scheme is based on generating a trajectory for the translational motion based on given waypoints in an inertial coordinate frame, and then obtaining the desired control force vector to asymptotically stabilize the desired translational motion trajectory. This desired control force vector direction is then used to generate a desired attitude trajectory. To track this desired attitude trajectory, a finite-time stable attitude tracking scheme is developed and used. The overall (integrated) trajectory generation and control scheme is simulated numerically, using a Lie group variational integrator to discretize this scheme for computer implementation. These numerical results show the stable performance of this integrated guidance and trajectory tracking control scheme. Future work will look at robustness to disturbance inputs acting on the dynamics and finite-time stability of the translational motion tracking scheme.

Acknowledgments The authors wish to thank Taeyoung Lee for helpful discussions on control of quadcopter UAVs, and with Jan Bohn for useful inputs on finite-time stable control on the Lie group of rigid body motions.

References

1. Aguiar, A.P., Hespanha, J.P.: Position tracking of underactuated vehicles. In: American Control Conference (ACC), 2003, vol. 3. IEEE, pp. 1988–1993 (2003)
2. Baviskar, A., Feemster, M., Dawson, D., Xian, B.: Tracking control of an underactuated unmanned underwater vehicle. In: American Control Conference (ACC), vol. 2005, pp. 4321–4326. IEEE (2005)
3. Bhat, S., Bernstein, D.: Finite-time stability of continuous autonomous systems. SIAM J. Control. Optim. **38**(3), 751–766 (2000)
4. Bloch, A.M., Baillieul, J., Crouch, P., Marsden, J.: Nonholonomic Mechanics and Control, ser. Interdisciplinary Texts in Mathematics. Springer, Verlag (2003)
5. Bohn, J., Sanyal, A.K.: Almost global finite-time stabilization of rigid body attitude dynamics using rotation matrices International Journal of Robust and Nonlinear Control (2015)
6. Bonnabel, S., Martin, P., Rouchon, P.: Non-linear symmetry-preserving observers on Lie groups. IEEE Trans. Autom. Control **54**(7), 1709–1713 (2009)
7. Bullo, F., Lewis, A.D.: Geometric Control of Mechanical Systems, ser. Texts in Applied Mathematics. Springer, Verlag (2004)
8. Casau, P., Sanfelice, R.G., Cunha, R., Cabecinhas, D., Silvestre, C.: Global trajectory tracking for a class of underactuated vehicles. In: American Control Conference (ACC), 2013. IEEE, pp. 419–424 (2013)
9. Hua, M., Hamel, T., Morin, P., Samson, C.: Introduction to feedback control of underactuated VTOL vehicles. IEEE Control. Syst. Mag. **33**(1), 61–75 (2013)
10. Izadi, M., Sanyal, A.K., Barany, E., Viswanathan, S.P.: Rigid body motion estimation based on the Lagrange-d'A,lembert principle. In: 54th IEEE Conference on Decision and Control (CDC), pp. 3699–3704 (2015)
11. Izadi, M., Sanyal, A.K., Beard, R., Bai, H.: GPS-denied relative motion estimation for fixed-wing UAV using the variational pose estimator. In: 54th IEEE Conference on Decision and Control (CDC), pp. 2152–2157 (2015)
12. Kobilarov, M.: Trajectory tracking of a class of underactuated systems with external disturbances. In: American Control Conference (ACC), 2013, pp. 1044–1049 (2013)
13. Lee, T., Leok, M., McClamroch, N.H.: Dynamics of connected rigid bodies in a perfect fluid. IEEE, 408–413 (2009)

14. Lee, T., Leok, M., McClamroch, N.H.: Geometric tracking control of a quadrotor UAV on SE(3). In: 49th IEEE Conference on Decision and Control (CDC). IEEE, pp. 5420–5425 (2010)
15. Leishman, R.C., McLain, T.W., Beard, R.W.: Relative navigation approach for vision-based aerial GPS-denied navigation. J. Intell. Robot. Syst. **74**(1-2), 97–111 (2014)
16. Leonard, N.E.: Periodic forcing, dynamics and control of underactuated spacecraft and underwater vehicles. In: 34th IEEE Conference on Decision and Control (CDC), vol. 4. IEEE, pp. 3980–3985 (1995)
17. Mellinger, D., Michael, N., Kumar, V.: Trajectory generation and control for precise aggressive maneuvers with quadrotors. Int. J. Robot. Res. **31**(5), 664–674 (2012)
18. Nordkvist, N., Sanyal, A.K.: A lie group variational integrator for rigid body motion in SE(3) with applications to underwater vehicle dynamics. In: 49th IEEE Conference on Decision and Control (CDC), pp. 5414–5419 (2010)
19. Pucci, D., Hamel, T., Morin, P., Samson, C.: Nonlinear feedback control of axisymmetric aerial vehicles. Automatica **53**, 72–78 (2015)
20. Rehbinder, H., Ghosh, B.K.: Pose estimation using line-based dynamic vision and inertial sensors. IEEE Trans. Autom. Control **48**(2), 186–199 (2003)
21. Sanyal, A., Holguin, L., Viswanathan, S.: Guidance and control for spacecraft autonomous chasing and close proximity maneuvers (2012)
22. Sanyal, A., Nordkvist, N., Chyba, M.: An almost global tracking control scheme for maneuverable autonomous vehicles and its discretization. IEEE Trans. Autom. Control **56**(2), 457–462 (2011)
23. Tabuada, P., Lima, P.: Position tracking for underactuated rigid bodies on SE(3), ISR Internal Report RT-401-2000, Tech Rep. (2000)
24. Tayebi, A., McGilvray, S.: Attitude stabilization of a VTOL quadrotor aircraft. IEEE Trans. Control Syst. Technol. **14**(3), 562–571 (2006)
25. Varadarajan, V.S.: Lie Groups, Lie Algebras, and Their Representations. Springer Verlag, New York (1984)
26. Vasconcelos, J.F., Cunha, R., Silvestre, C., Oliveira, P.: A nonlinear position and attitude observer on SE(3) using landmark measurements. Syst. Control Lett. **59**(3), 155–166 (2010)

Sasi Prabhakaran Viswanathan is a CEO and founder at Akrobotix LLC, a Genius NY company. He received his B.E., degree in mechanical engineering from Government College of Technology, Tamil Nadu, India, in 2008. He held the research fellow position at the Indian Institute of Science, Bangalore and Indian Institute of Technology, Mumbai during 2008 and 2010, respectively. He graduated with M.S. and Ph.D., degrees in mechanical engineering in 2012 and 2015, respectively from New Mexico State University. After graduating with the doctorate, he carried out the research activities in the area of autonomous unmanned systems as a postdoctoral research associate in the department of mechanical and aerospace engineering at Syracuse University. Dr. Prabhakaran's research interest includes multibody dynamics, nonlinear system and control, system engineering, robotics, and mechatronics.

Amit K. Sanyal received a B.Tech. in aerospace engineering from the Indian Institute of Technology, Kanpur, in 1999 and M.S. in aerospace engineering from Texas A&M University in 2001. He received the M.S. in mathematics and Ph.D. in aerospace engineering from the University of Michigan in 2004. From 2004 to 2006, he was a postdoctoral research associate in the Mechanical and Aerospace Engineering department at Arizona State University. From 2007 to 2010, he was an Assistant Professor in Mechanical Engineering at the University of Hawaii, and from 2010 to 2015 he was in the Mechanical and Aerospace engineering department at New Mexico State University. He is currently Associate Professor in Mechanical and Aerospace engineering at Syracuse University. His research interests are in geometric mechanics, geometric control, discrete variational mechanics for numerical integration of mechanical systems, optimal control and estimation, geometric/algebraic methods applied to nonlinear systems, spacecraft guidance and control, and control of unmanned vehicles. He is a member of the IEEE Control Systems Society technical committees on Aerospace Control and Nonlinear Control, and past member of the AIAA Guidance, Navigation, and Control Technical Committee.

Ehsan Samiei received a B.E. degree in electrical engineering from Shahid Rajaee University, Tehran, Iran in 2006 and M.S. in electrical engineering-control systems from Amirkabir University (Tehran polytechnic), Tehran, Iran in 2009. He received his Ph.D. degree in aerospace engineering with minor in mechanical engineering in 2015 from New Mexico State University. He is currently an advanced research engineer at Delphi Automotive PLC designing and developing self-driving vehicles. His research primarily focuses on control systems design, including theoretical and computational aspects of nonlinear and geometric control, control of attitude motion, artificial intelligence-based control design, and time delay and stochastic control systems. He is especially interested in applications to spacecraft control systems and autonomous vehicles.